applied optics

Polarizing grating color filters with large acceptance angle and high transmittance

Zhenyue Luo,[1] Guiju Zhang,[2] Ruidong Zhu,[1] Yating Gao,[1] and Shin-Tson Wu[1,*]

[1]CREOL, The College of Optics and Photonics, University of Central Florida, Orlando, Florida 32816, USA
[2]Institute of Modern Optical Technologies, Soochow University, Suzhou 215006, China
*Corresponding author: swu@ucf.edu

Received 21 September 2015; revised 23 November 2015; accepted 25 November 2015; posted 25 November 2015 (Doc. ID 250437); published 22 December 2015

We design and simulate a polarizing color filter with a sub-wavelength metal-dielectric grating. It manifests several advantages: a large acceptance angle (up to ±50°), high transmittance (74.3%–92.7%), low absorption loss (~3.3%), and a high extinction ratio. This polarizing color filter can be integrated into a liquid-crystal display (LCD) backlight system to simultaneously recycle the light according to its color and polarization. In combination with a specially designed directional backlight, this newly proposed LCD system can theoretically improve optical efficiency up to ~2.5×, and also provides a large ambient contrast ratio and a wide view. Our approach enables an ultra-low-power LCD without using the complicated field-sequential-color technique.

OCIS codes: (230.3720) Liquid-crystal devices; (050.6624) Subwavelength structures; (260.5430) Polarization.

http://dx.doi.org/10.1364/AO.55.000070

1. INTRODUCTION

Power consumption is a critical issue for all kinds of liquid-crystal displays (LCDs), such as smartphones, computers, and TVs [1]. For an LCD, two major components affecting the power consumption are polarizers and color filters. Most of the high-contrast, full-color LCDs employ two crossed polarizers and spatial color filters (CFs). A linear polarizer absorbs about one half, while each CF absorbs more than two-thirds of the incident backlight, such as a white LED (light-emitting diode). As a result, the total optical efficiency of an LCD system is only about 5%–7%.

To reduce the optical loss of polarizers, one can utilize a linearly polarized LED light source [2] or incorporate a reflective polarizer to recycle the unused polarization [3–6]. A reflective polarizer transmits one polarization while reflecting the other. It can introduce polarization recycling within the backlight and thereby enhance the light efficiency by ~60%. Two examples of reflective polarizers are 3M's dual brightness enhancement film [3], and the wire grid polarizer (WGP) [4–6]. However, both devices cannot reduce the light loss in color filters.

To eliminate spatial color filters, one could consider a temporal field-sequential-color (FSC) technique. However, the FSC demands a fast liquid crystal (LC) response time (<1 ms) to suppress the color breakup, which is still challenging for nematic LCDs [7,8]. An angular color separation backlight [9,10] has also been proposed to reduce the optical loss of color filters. It uses a specially designed grating to angularly separate the light according to its wavelength. Each red, green, or blue beam then passes through a matched color filter with little loss. However, this technique requires several optical elements, e.g., a grating and microlens structures, etc., to collimate the light. Thus, the display system is complicated. Moreover, due to the angular separation, the output angle for each color does not overlap. This effect introduces a significant color shift.

Recently, grating-based color filters have received a great deal of attention [11–23]. Instead of using absorptive pigments, these grating-based color filters separate colors via diffraction, interference, or the surface plasmon effect. The light outside the transmission band is reflected instead of being absorbed. Therefore, this device is highly energy efficient. The grating CF array can also have a high density and is resistant to material degradation. As a result, they are attractive for various applications, including solar cells [11], image sensors [12], and reflective displays [13,14]. However, most grating CFs are angular sensitive, and they require complex optics to collimate the incident light [15–17]. This drawback severally limits their applications. Although some reflective grating CFs with much reduced angular sensitivity have been recently proposed [13,14], the transmission-type grating CF with a high transmittance and large angular tolerance remains a technical challenge. For a wide-view transmissive LCD, normally, the backlight has a quasi-Lambertian distribution; therefore, we cannot directly apply the grating CF in the backlight system.

In this paper, we propose a new grating CF design with a large angular tolerance and high transmittance. This grating CF can replace the bottom polarizer and the absorptive pigment CFs in conventional LCDs. It only transmits the light with the desired polarization and colors, while reflecting the rest for recycling. Thus, the backlight system can simultaneously recycle the light according to its color and polarization. As a result, the optical efficiency of the LCD can be enhanced by ~2.5×. We can also combine this grating CF with directional backlight to achieve a high ambient contrast ratio, wide viewing angle, and low power consumption. Our approach offers a simple solution for ultra-low-power LCDs without the sophisticated FSC technique.

2. GRATING COLOR FILTER DESIGN

We first describe the grating-based polarizing CF, which has dual functions as a linear polarizer and a color filter. Figure 1(a) shows the device structure. The flexible PMMA structure ($n = 1.48$) is first coated with a thin layer of magnesium fluoride (MgF_2) with a thickness of $h_1 = 40$ nm, and then is covered by a compound grating of aluminum (Al) and MgF_2 with a thickness of $h_2 = 100$ nm. Different CFs have different grating periods Λ and duty cycles f. After the iterative parameter scan [16], we obtained the following geometrical parameters for each CF: ($\Lambda = 150$ nm, $f = 0.76$) for blue, ($\Lambda = 110$ nm, $f = 0.86$) for green, and ($\Lambda = 110$ nm, $f = 0.92$) for red.

We simulated the grating's optical performance with the Gsolver V5.2 [24], an electro-magnetic simulation software based on the rigorous coupled-wave analysis (RCWA) [25,26]. The RCWA is a rigorous solution to the full-vector Maxwell's equations, except for the truncation of the Fourier expansion when a numerical simulation is performed. We can achieve the RCWA's numerical convergence by including a sufficient number of diffraction orders. The RCWA also allows us to examine the diffraction efficiency of each diffraction order. From the simulation results, we found that the zeroth-order diffracted wave is dominant. This is because our grating structure is sub-wavelength, so only a zeroth-order diffracted wave can propagate, while higher-order diffracted waves become evanescent [20].

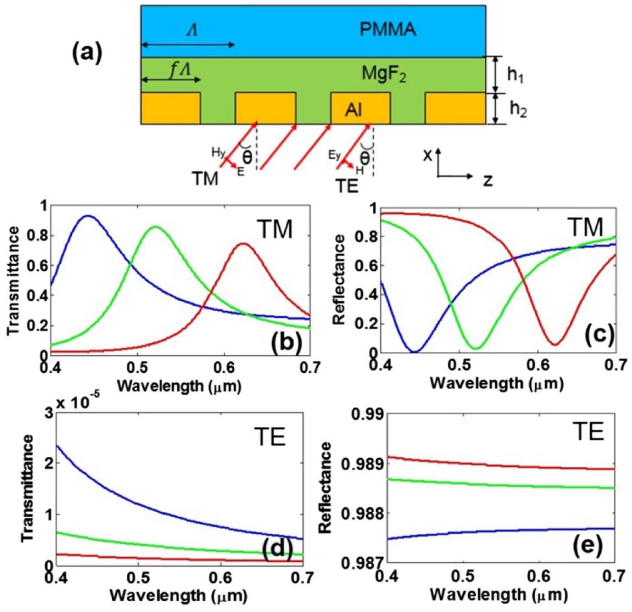

Fig. 1. (a) Schematic drawing of the proposed grating structure. (b) Simulated TM transmission spectrum for RGB grating CFs. (c) TM reflection spectrum. (d) TE transmission spectrum. (e) TE reflection spectrum.

A typical LCD pixel size is around 8–50 μm [1], while the sub-wavelength grating period is ≤150 nm; therefore each pixel corresponds to a grating with >50 grating periods. With such a large number of grating periods, we can safely apply the RCWA without considering the effect of a finite grating period [26].

In the simulation, the dispersion information associated with Al was derived from the Lorentz–Drude model [27]. MgF_2 was assumed to have a constant refractive index of 1.38 with a negligible optical loss, while the PMMA substrate has a constant refractive index of 1.48. The RCWA simulation is performed for the transverse electric (TE) and transverse magnetic (TM) input waves separately. As Fig. 1(a) shows, the TE and TM waves have an electric field and magnetic field parallel to the grating orientation (y direction), respectively.

Figure 1(b) depicts the TM transmission spectra for the blue, red, and green CFs. The transmission spectra are normalized to the input fields. They exhibit evident color-filtering properties. The peak transmissions for the blue, red, and green CFs are 92.7%, 84.7%, and 74.3%, respectively. This unmatched peak transmission could be attributed to the dispersion property of Al. In the blue region, Al shows a metallic-like behavior and acts as a low-loss plasmonic material, while in the red region, the imaginary part of the dielectric constant increases, which leads to decreased transmittance. A more detailed explanation can be found in [24]. Figure 1(c) shows the simulated TM reflection spectra. It exhibits a reflection dip, which is like a reversal to the transmission spectra. By adding the reflectance and transmittance together, we find that the grating structure has very little absorption loss (~3.3%) for the TM light. Most of TM-polarized light is either transmitted or reflected for recycling.

The TE reflection and transmission spectra are also shown in Figs. 1(d) and 1(e). They have a fairly low transmittance to TE light. The extinction ratios (the ratio of TE/TM wave transmission, i.e., $E_{xt} = T_{TE}/T_{TM}$) for red, green, and blue (RGB)-polarizing CFs are 4.2E4, 1.0E5, and 1.8E5, which are much larger than that of commercial sheet polarizers (~6E3) [1]. Therefore, this polarizing CF could replace the commercial sheet polarizers employed in LCDs to further improve the contrast ratio.

A common issue with the grating CF is its tight angular tolerance. For most optical gratings, the color-filtering property originates from light diffraction and interference on the periodic structure. Thus, it highly depends on the light's incident angle. Several one-dimensional (1D) grating CF designs have been studied previously [15–17]. However, all of them exhibited a very strict angular tolerance (<10°), i.e., they showed a substantial color variation when viewed slightly off-axis. In a normal edge-lit LCD backlight system, the light distribution is around the ±50° ~ 60° cone angle. Therefore, the previously proposed structure cannot be used in LCD backlighting.

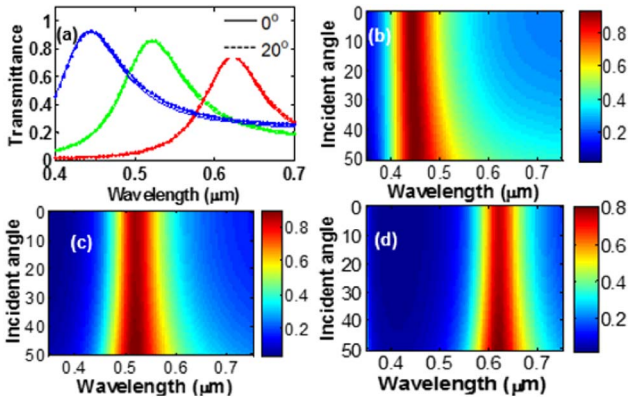

Fig. 2. (a) TM transmission for light incident at 0° and 20°. (b), (c), and (d) The transmission spectra versus the incident angle for the blue, green, and red polarizing CFs, respectively.

On the contrary, our proposed polarizing CF manifests a low angular sensitivity. Figure 2(a) compares the TM transmission spectra for the light incident at 0° and 20°. Their difference is very small. Figures 2(b), 2(c), and 2(d) further show the transmission spectra versus the incident angle for the R, G, and B polarizing CFs. As the light incident angle increases from 0° to 50°, both the peak transmission wavelength and the full width at half-maximum (FWHM) of the transmission band are almost the same. This angular independence is an important advantage of our proposed design. It can be used in an LCD backlight without introducing angular-dependent color variation.

To understand the origin of this unusual transmission performance, we simulated the light field distribution inside the blue polarizing CF. Figure 3(a) plots the TE field distribution.

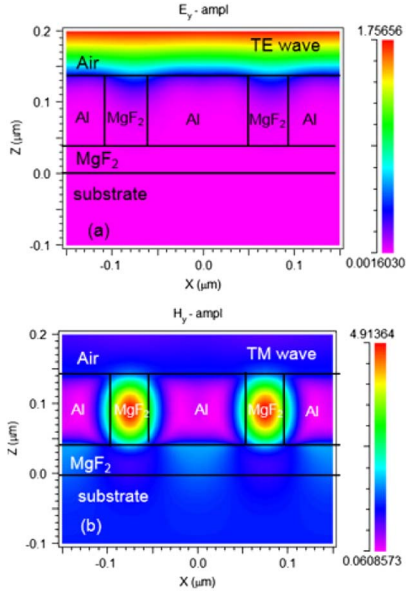

Fig. 3. Simulated field distribution of $\lambda = 450$ nm at a normal incidence in the blue polarizing CF. (a) Electric field for TE wave. (b) Magnetic field for TM wave. The light is incident from the air side.

Table 1. Comparison of Our Grating CF Design with Previously Published Results

	Structure	FWHM (nm)	Peak T (%)	Angular Tolerance (°)
[15,16]	1D grating	~110	70–80	<10
[18]	2D grating	~60	40–60	30 ~ 40
[19]	MDM stack	~150	25	60 ~ 70
This work	1D grating	~110	75 ~ 90	~50

The light incident from the air side cannot penetrate into the grating structure due to surface plasmon excitation [6,20], and is therefore reflected. As a result, the polarizing CF exhibits an excellent extinction ratio for TE transmission.

On the other hand, the TM wave in Fig. 3(b) manifests strong localized Fabry–Perot cavity resonance inside the MgF_2 slits. Most of the field is confined within the dielectric slits; only a tiny portion is extended into the metal region. By leaking through the dielectric slits, the incident TM wave can transmit the grating with a low absorption loss.

In a typical grating-based color filter, there are two types of resonance effects that lead to color filtering behavior [22]: (1) the grating resonance, i.e., the constructive interference from a periodic structure. This grating resonance is strongly dependent on the incident angle [15–17]. (2) Localized Fabry–Perot resonance [21,22], i.e., the result of standing wave formation from the two counter propagating waves in the metal-dielectric-metal slits. This Fabry–Perot resonance is strongly related to the slits' depths and widths, as well as the index match between the metal/dielectric materials, and is less dependent on the incident angle. Our structure filters the light by Fabry–Perot resonance, and therefore has a relatively large angular tolerance.

Table 1 compares the optical performance of several transmission-type grating CFs in terms of FWHM, peak transmission, and angular tolerance. A typical 1D grating [15,16] has iridescent light transmission and is very sensitive to the incident angle. A 2D plasmonic grating with cross-holes [18] and a 1D metal-dielectric-metal (MDM) stack [19] manifest wide-angle color filtering properties, but their peak transmission is fairly low. Moreover, both structures are difficult to fabricate by nano-patterning for large area. Some angle-insensitive reflective grating CFs were also proposed [14], but they are based on omnidirectional light absorption and therefore cannot be utilized for transmissive display applications.

Compared to previous designs, our polarizing CFs possess several attractive properties: high transmittance (74.3%–92.7%), low absorption loss (~3.3%), a high extinction ratio (>1E4), and a large angular tolerance (up to ±50°). Moreover, the proposed polarizing CF is a typical 1D grating whose geometric features are similar to those of the WGP. The WGP has been commercialized and can be fabricated using several approaches, such as interference lithography, nano-imprinting, and the roll-to-roll process [5,17,19]. These mature technologies can also be employed to pattern the polarizing CF on a large scale with low cost.

3. LCD SYSTEM DESIGN

Our polarizing CF has a large angular tolerance and can be directly applied in the LCD backlight. However, a typical edge-lit LCD backlight with a light guide plate (LGP) and crossed brightness enhancement films has a large output cone angle of ±50° – 60°. To further mitigate the angular-dependent color variation, here, we propose to combine the polarizing CF with directional backlighting [28].

Figure 4 depicts the schematic diagram of the newly proposed LCD system. It consists of an LED light source, a directional LGP, a polarizing CF, and an LCD panel, as well as a top-engineered diffuser. Here, the directional LGP is a key element. It extracts the LED light by its bottom microstructure, and then collimates the light by the microlens on its top surface, as shown in Fig. 4. Therefore, the light entering the LCD panel is relatively collimated, which is essential for improving the LCD's contrast ratio and reducing the color shift [28–32].

After the light exits the LC panel, it is spread out by the top diffuser to achieve a wide view. The top diffuser is like an inverted microlens array [31]. The light is focused on the central area of each microlens, and then diffused into a large cone angle. In this way, the LCD can provide a wide view, high contrast ratio, and an indistinguishable color shift. For a sunlight-readable display, the ambient light is reflected from the device surface as noise, which in turn degrades the contrast ratio. To reduce surface reflection, we can deposit a black matrix on top of the diffuser. As Fig. 4 shows, the top diffuser focuses the light into a small area; thus, the remaining ~80% unused area can be covered with a black matrix without sacrificing the LCD transmittance. This black matrix absorbs the ambient light and enhances the ambient contrast ratio. More detailed information on the directional backlight and diffuser has been provided in [28,31].

We simulated such an LCD system with the non-sequential ray tracing software LightTools 8.0 [33]. Figure 5(a) shows the light angular distribution before it impinges on the LC cell. The directional LGP collimates the backlight to ±10° cone angle. Figure 5(b) plots the angular light intensity distribution after the light passes through the top diffuser. Light is scattered to a much wider cone angle to ensure a wide view. We also calculated the ambient reflection, which is only ~2%. Therefore, the display should exhibit a high ambient contrast ratio.

To understand the superiority of the proposed directional backlight, we performed an optical analysis by an integral

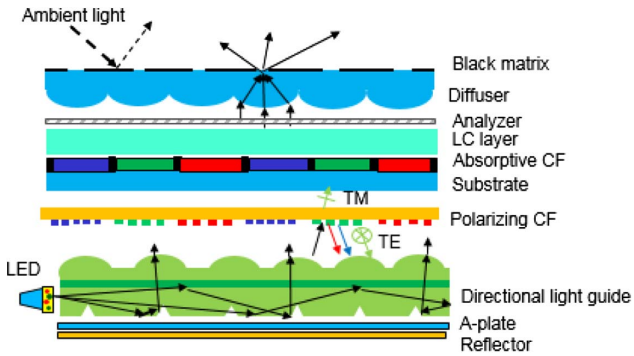

Fig. 4. Device structure of the proposed backlight system.

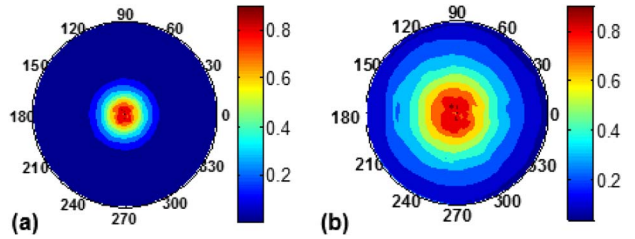

Fig. 5. (a) Simulated light intensity angular distribution of the backlight before it enters the LCD panel. (b) Angular distribution after the light is diffused by the top diffuser. The light intensity is normalized to the peak light intensity in the on-axis direction.

geometrical optics/wave optics simulation [28]. Without losing generality, we consider the single-domain vertical aligned (VA) LCD mode [34]. The LC material is Merck MLC-6882 ($\Delta n = 0.097$ and $\Delta\varepsilon = -3.1$), and cell gap is 4 μm. The resultant on-state voltage is ~5.1 V_{rms}, and the response time is ~10 ms. The LC pre-tilt angle is 1° along the 135° azimuthal direction. The single-domain VA mode is difficult to achieve in the wide view; thus a multi-domain structure with compensation films has to be used [35,36]. To show the advantage of the proposed directional backlight design, here, we use a single-domain VA without any compensation film as an example. We calculated the contrast ratio [1] (the transmittance ratio in the voltage on/off states). Figures 6(a) and 6(b) show the simulated isocontrast contour of the single-domain VA LCD with conventional backlight and directional backlight, respectively. In Fig. 6(a), the high contrast ratio (CR) region is limited to a ~20° viewing cone, while in Fig. 6(b), CR > 100:1 extends to 80°. If we add compensation films, then the isocontrast of CR = 3000:1 would cover the entire 80° viewing cone [28].

Figures 6(c) and 6(d) plot the gamma curves of the single-domain VA LCD at different viewing angles. With

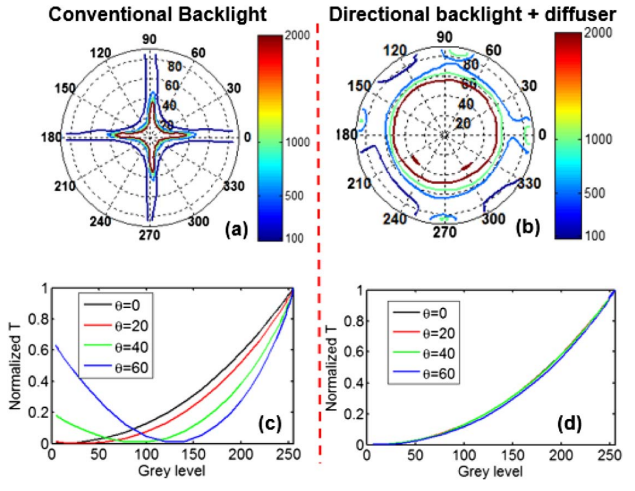

Fig. 6. Simulated isocontrast contours of single-domain VA LCD with (a) conventional backlight and (b) directional backlight + engineered diffuser. Gamma curve of VA LCD with (c) conventional backlight and (d) directional backlight + engineered diffuser. The azimuthal angle is 45°, and no compensation film is included in the LCD system.

conventional backlight [Fig. 6(c)], the LCD suffers from serious grayscale inversion even at a relatively small viewing angle. But with directional backlight, the gamma curves are almost indistinguishable [Fig. 6(d)] from the 0° to 60° viewing angles. This means that the image quality remains almost the same at different viewing angles.

The majority of present LCD TVs employ a multi-domain vertical alignment (MVA) structure because it exhibits a high contrast ratio and wide viewing angle [35,36]. Although MVA has achieved tremendous success, it still has some drawbacks: (1) some dead zones exist between different domains, which lowers the transmittance, and (2) its color shift and gamma shift are still noticeable. Our proposed LCD backlight enables a wide view by using a simple single-domain VA LCD. Therefore, it helps reduce the LC panel fabrication cost while improving the optical efficiency and image quality.

As discussed in Section 2, the proposed polarizing CF has angular tolerance of ±50°. Since the specially designed LGP collimates the backlight to the ±10° cone, we can safely apply the polarizing CF in the LCD system without worrying about the color shift.

As Fig. 4 indicates, the polarizing CF is sandwiched between the LC panel and the directional backlight. Each polarizing color filter, say, green, only transmits TM polarization with the green color, while reflecting the other TM light outside the green band as well as all the TE polarization. The reflected light is recycled within the backlight system. In Fig. 4, we intentionally laminate one anisotropic A-plate on top of the bottom reflector to enhance the polarization conversion. The system optical efficiency is enhanced as the recycled TE wave is partially converted to TM. Moreover, during recycling, the reflected TM light with a different color has the potential to transmit through other appropriate polarizing CFs, e.g., red and blue. Thus, the polarizing CFs redistribute the light output with an appropriate polarization and color, and significantly reduce the light loss due to polarization or color mismatch.

As Fig. 2(b) shows, the polarizing CF has a relatively broad transmission band that may induce color crosstalk. This issue should be taken into consideration in the LCD backlight system design. To ensure good color purity, we could employ either RGB LEDs or quantum-dot-enhanced white LEDs [37–39] as the light source. Figure 7 depicts the emission spectrum (black solid lines) of a quantum dot backlight.

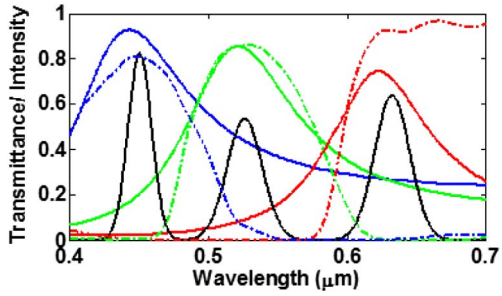

Fig. 7. Light source spectrum (black solid line), transmission spectra of polarizing CF (R/G/B solid lines), and transmission spectra of absorptive CFs (R/G/B dashed–dotted lines).

The emission bandwidth is relatively narrow, thus, they are less affected by the polarizing CFs. To further ensure good color purity, we can keep the spatial color filters after the polarizing CF (Fig. 4). The transmission spectra of the absorptive CFs are shown as dashed lines in Fig. 7. They match well with those of polarizing CFs (solid lines). Even though the absorptive CF is employed, the polarizing CFs have already redistributed the output light with different colors to match the transmission band of the absorptive CFs. Therefore, the optical loss introduced by the absorptive CFs is minimal.

Another important concern for LCD backlight is whether the light recycling would deteriorate the color collimation behavior. Since our employed diffractive optical element is a sub-wavelength structure, it only propagates the zeroth-order diffracted wave. Thus, the light propagation behavior can still be modeled by ray optics. We tested the angular distribution of the directional LGP after several light propagating cycles in LightTools, and found that the light is still well collimated. The loss during each recycle is less than 10%. This is because the directional LGP does not contain any absorptive or diffusive microstructure.

4. OPTICAL PERFORMANCE

By combining the polarizing CF with an LCD system, we can obtain several advantages: high contrast, wide view, low ambient light reflection, and mitigated angular-dependent color variation. The most significant benefit is the optical gain due to light recycling. Here, we derive an analytical equation to calculate the optical gain.

Let us assume an unpolarized light source consisting of 50% TE and 50% TM waves. Without losing generality, we first consider the propagation behavior of blue light in the backlight system. We also define the blue, green, and red polarizing CFs as having a transmission of (T_1, T_2, T_3) and reflection of (R_1, R_2, R_3), respectively, for the TM wave, and zero transmission and unity reflection for the TE wave.

When the blue light first impinges on the polarizing filter array, there is a 1/3 probability that it will transmit through the blue CF, i.e., the matched one. There is also a 2/3 probability that it will hit the green or red filter (the unmatched CF). Although some blue light may still transmit through the unmatched polarizing CF, it will be absorbed by the subsequent absorptive CFs and does not contribute to the display brightness. As a result, only the TM wave hitting the blue CF can transmit. The transmission ratio is $T_1/6$. On the other hand, the reflection upon the first hit consists of all the reflected TE and reflected TM waves from the unmatched filters. Therefore, the total reflection is $1/2 + (R_2 + R_3)/6$.

The reflected light is recycled within the backlight system. We assume during each light recycling that the light intensity would be reduced by a factor of T. When the light is incident on the polarizing CF for the second time, its transmittance is equal to $[1/2 + (R_2 + R_3)/6] * T$. We also assume the light becomes completely unpolarized after the recycling. This is an idealized assumption that sets the best scenario for our estimation. Similar to our previous analysis, the ratio of light that can transmit the second time is $T_1/6 * [1/2 + (R_2 + R_3)/6]T$, and the ratio of light reflection is $[\mathrm{T}/2 + (R_2 + R_3)/6]^2 T$.

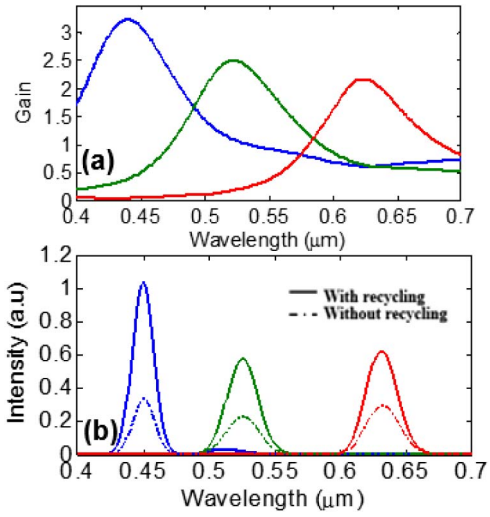

Fig. 8. (a) Simulated optical gain for RGB grating CFs. (b) Backlight output intensity with and without recycling.

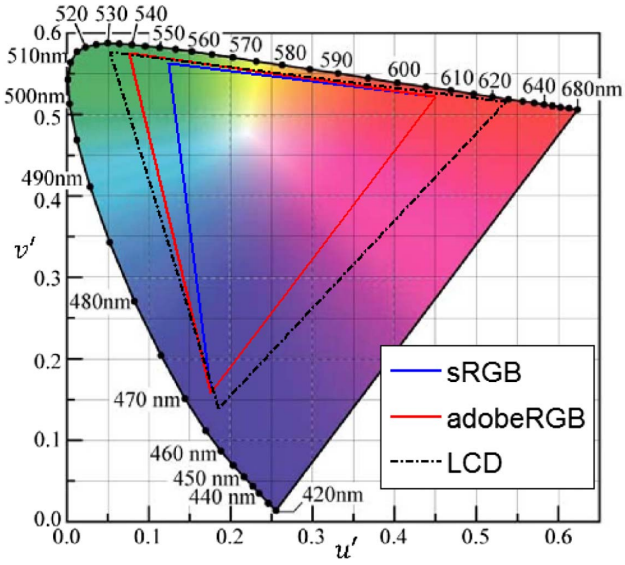

Fig. 9. Color gamut of LCD (with directional backlight and polarizing CF) in the CIE 1976 color space.

This iteration repeats, and we can sum up all the transmission terms and obtain the total output transmittance as

$$T_{\text{out}} = \frac{1}{6}T_1 + \left(\frac{1}{6}(R_2+R_3)+\frac{1}{2}\right)T * \frac{1}{6}T_1 + \left(\frac{1}{6}(R_2+R_3)+\frac{1}{2}\right)^2 T^2 * \frac{1}{6}T_1 + \ldots = \frac{T_1/6}{1-\left[\frac{1}{2}+\frac{R_2+R_3}{6}\right]T}. \quad (1)$$

On the other hand, without applying polarizing CF, the light from backlight has a 1/6 probability of reaching the LC panel (1/2 from the absorptive polarizers, and 1/3 from the absorptive pigment CFs). Therefore, after introducing the polarization and color recycling, we can obtain the optical gain factor G as

$$G = \frac{T_1}{1-\left[\frac{1}{2}+\frac{R_2+R_3}{6}\right]T}. \quad (2)$$

According to Eq. (2), a high transmission for matched color (T_1), high reflection for unmatched color (R_2, R_3), and a high backlight factor (T) are the key factors for achieving a high optical gain, G.

Next, let us assume the backlight has a ~10% recycling loss ($T = 0.9$), which matches with the LightTools simulation. Using the reflection and transmission spectra (Fig. 7) in Eq. (2), we can obtain the gain spectrum for RGB polarizing CFs. Figure 8(a) plots the simulated optical gain. Each polarizing CF provides a large optical gain (2.2 × ~3 ×) for the light at the peak transmission wavelength. In particular, the blue polarizing CF exhibits the largest optical gain (~3×), while the red polarizing CF has a slightly lower gain (~2.2×) due to the lower grating transmission.

We also calculate the light output spectrum by considering the absorptive CF spectrum and quantum-dot (QD) light source spectrum. Figure 8(b) shows the calculation results. The LCD output intensity spectra with and without light recycling are shown by the dashed lines and solid lines, respectively. It is evident that the light intensities of all three colors are enhanced by 2–3 ×.

The light output from each color channel also maintains excellent color purity after recycling. Figure 9 plots the color gamut in the CIE1976 color space. The LCD covers ~132% of the AdobeRGB region. Therefore, the light efficiency is enhanced without sacrificing the color performance.

5. CONCLUSION

In summary, we propose a directional LCD backlight system that can simultaneously recycle light according to its color and polarization. To the best of our knowledge, this is the first time that such a concept has been proposed. A novel polarizing CF is also designed, and it exhibits several advantages: high transmittance (74.3%–92.7%), low absorption loss (~3.3%), a high extinction ratio (>10, 000:1), and a large angular tolerance (up to ±50°). Combined with the directional backlight design, the proposed LCD system can achieve a ~2.5× system efficiency enhancement, as well as a high ambient contrast ratio and wide view. Our approach has potential applications for ultra-low-power LCDs without using the complicated field sequential color technique.

Funding. Air Force Office of Scientific Research (AFOSR) (FA9550-14-1-0279).

REFERENCES

1. M. Schadt, "Milestone in the history of field-effect liquid crystal displays and materials," Jpn. J. Appl. Phys. **48**, 03B001 (2009).
2. Z. Luo, Y. Cheng, and S. T. Wu, "Polarization-preserving light guide plate for a linearly polarized backlight," J. Disp. Technol. **10**, 208–214 (2014).
3. Y. Li, T. X. Wu, and S. T. Wu, "Design optimization of reflective polarizers for LCD backlight recycling," J. Disp. Technol. **5**, 335–340 (2009).

4. Z. B. Ge and S. T. Wu, "Nanowire grid polarizer for energy efficient and wide-view liquid crystal displays," Appl. Phys. Lett. **93**, 121104 (2008).
5. S. H. Ahn, J. S. Kim, and L. J. Guo, "Bilayer metal wire-grid polarizer fabricated by roll-to-roll nanoimprint lithography on flexible plastic substrate," J. Vac. Sci. Technol. B **25**, 2388–2391 (2007).
6. A. Lehmuskero, B. Bai, P. Vahimaa, and M. Kuittinen, "Wire-grid polarizers in the volume plasmon region," Opt. Express **17**, 5481–5489 (2009).
7. T. Takahashi, H. Furue, M. Shikada, N. Matsuda, T. Miyama, and S. Kobayashi, "39.1: A field-sequential-color matrix display using polymer-stabilized FLCD cells," SID Symp. Dig. Tech. Pap. **30**, 858–861 (1999).
8. Z. Luo and S. T. Wu, "A Spatiotemporal four-primary color LCD with quantum dots," J. Disp. Technol. **10**, 367–372 (2014).
9. J. Kimmel, "Review paper: Diffractive backlight technologies for mobile applications," J. Soc. Inf. Disp. **20**, 245–258 (2012).
10. P. C. Chen, H. H. Lin, C. H. Chen, C. H. Lee, and M. H. Lu, "Color separation system with angularly positioned light source module for pixelized backlighting," Opt. Express **18**, 645–655 (2010).
11. W. Long, Q. Chen, S. Song, Y. Yu, L. Jin, and X. Hu, "Photon harvesting, coloring and polarizing in photovoltaic cell integrated color filters: Efficient energy routing strategies for power-saving displays," Nanotechnology **26**, 265203 (2015).
12. S. Yokogawa, S. P. Burgos, and H. Atwater, "Plasmonic color filters for CMOS image sensor applications," Nano Lett. **12**, 4349–4354 (2012).
13. C. Yang, W. Shen, Y. Zhang, K. Li, X. Fang, X. Zhang, and X. Liu, "Compact multilayer film structure for angle insensitive color filtering," Sci. Rep. **5**, 9285 (2015).
14. K. Lee, S. Seo, and L. J. Guo, "High-color-purity subtractive color filters with a wide viewing angle based on plasmonic perfect absorbers," Adv. Opt. Mater. **3**, 347–352 (2015).
15. Y. Kanamori, M. Shimono, and K. Hane, "Fabrication of transmission color filters using silicon subwavelength gratings on quartz substrates," IEEE Photon. Technol. Lett. **18**, 2126–2128 (2006).
16. Y. Ye, Y. Zhou, H. Zhang, and L. S. Chen, "Polarizing color filter based on a subwavelength metal-dielectric grating," Appl. Opt. **50**, 1356–1363 (2011).
17. Z. C. Ye, J. Zheng, S. Sun, L. D. Guo, and H. P. D. Shieh, "Compact transreflective color filters and polarizers by bilayer metallic nanowire gratings on flexible substrates," IEEE J. Sel. Top. Quantum Electron. **19**, 1077–1082 (2013).
18. R. Girard-Desprolet, S. Boutami, S. Lhostis, and G. Vitrant, "Angular and polarization properties of cross-holes nanostructured metallic filters," Opt. Express **21**, 29412–29424 (2013).
19. J. Y. Lee, K. T. Lee, S. Seo, and L. J. Guo, "Decorative power generating panels creating angle insensitive transmissive colors," Sci. Rep. **4**, 4192 (2014).
20. R. Halir, P. J. Bock, P. Cheben, A. Ortega-Monux, C. Alonso-Ramos, J. H. Schmid, J. Lapointe, D. X. Xu, J. G. Wanguemert-Perez, I. Molina-Fernandez, and S. Janz, "Waveguide sub-wavelength structures: a review of principles and applications," Laser Photon. Rev. **9**, 25–49 (2015).
21. R. Wu, A. E. Hollowell, C. Zhang, and L. J. Guo, "Angle-Insensitive structural colours based on metallic nanocavities and coloured pixels beyond the diffraction limit," Sci. Rep. **3**, 1194 (2013).
22. J. Zhou and L. J. Guo, "Transition from a spectrum filter to a polarizer in a metallic nano-slit array," Sci. Rep. **4**, 3614 (2014).
23. P. West, S. Ishii, G. Naik, N. Emani, V. Shalaev, and V. A. Boltasseva, "Searching for better plasmonic materials," Laser Photon. Rev. **4**, 795–808 (2010).
24. Gsolver 5.2, http://www.gsolver.com/.
25. M. G. Moharam, E. B. Grann, D. A. Pommet, and T. K. Gaylord, "Formulation for stable and efficient implementation of the rigorous coupled-wave analysis of binary gratings," J. Opt. Soc. Am. **12**, 1068–1076 (1995).
26. K. Hirayama, E. Glytsis, and T. Gaylord, "Rigorous electromagnetic analysis of diffraction by finite-number-of-periods gratings," J. Opt. Soc. Am. **14**, 907–917 (1997).
27. M. A. Ordal, L. L. Long, R. J. Bell, S. E. Bell, R. R. Bell, R. W. Alexander, Jr., and C. A. Ward, "Optical properties of the metals, Al, Co, Cu, Au, Fe, Pb, Ni, Pd, Pt, Ag, Ti and W in the infrared and far infrared," Appl. Opt. **22**, 1099–1119 (1983).
28. Y. Gao, Z. Luo, Z. Zhu, Q. Hong, S. T. Wu, M. C. Li, S. L. Lee, and W. C. Tsai, "A high performance single-domain LCD with wide luminance distribution," J. Disp. Technol. **11**, 315–324 (2015).
29. J. Pan and Y. Hu, "Design of a hybrid light guiding plate with high luminance for backlight system application," J. Disp. Technol. **9**, 965–971 (2013).
30. R. Zhu, Q. Hong, Y. Gao, Z. Luo, and S. T. Wu, "Tailoring the light distribution of liquid crystal display with freeform engineered diffuser," Opt. Express **23**, 14070–14084 (2015).
31. T. Teng and J. Ke, "A novel optical film to provide a highly collimated planar light source," Opt. Express **21**, 21444–21455 (2013).
32. X. Zhu, Z. Ge, and S.-T. Wu, "Analytical solutions for uniaxial-film-compensated wide-view liquid crystal displays," J. Display Technol. **2**, 2–20 (2006).
33. LightTools 8.3, http://optics.synopsys.com/lighttools/.
34. M. F. Schiekel and K. Fahrenschon, "Deformation of nematic liquid crystals with vertical orientation in electric fields," Appl. Phys. Lett. **19**, 391–393 (1971).
35. H. Seiberle and M. Schadt, "Photo-alignment and photo-patterning of planar and homeotropic liquid crystal display configurations," J. Soc. Inf. Disp. **8**, 67–71 (2000).
36. L. Jin, J. Sohn, H. Kim, and S. H. Lee, "Recent trends on patterned vertical alignment (PVA) and fringe-field switching (FFS) liquid crystal displays for liquid crystal television applications," J. Disp. Technol. **3**, 404–412 (2007).
37. N. P. J. Kurtin, B. Theobald, N. Stott, and J. Osinski, "Quantum dots for high color gamut LCD displays using an on-chip LED solution," SID Symp. Dig. Tech. Pap. **45**, 146–148 (2014).
38. Z. Luo, Y. Chen, and S.-T. Wu, "Wide color gamut LCD with a quantum dot backlight," Opt. Express **21**, 26269–26284 (2013).
39. Z. Luo, D. Xu, and S. T. Wu, "Emerging quantum-dots-enhanced LCDs," J. Disp. Technol. **10**, 526–539 (2014).